ROYAL SOCIETY OF CHEMISTRY

EDGE ARTICLE

CrossMark
← click for updates

Cite this: Chem. Sci., 2017, 8, 2574

Visible light-induced water splitting in an aqueous suspension of a plasmonic Au/TiO₂ photocatalyst with metal co-catalysts†

A. Tanaka,*[a] K. Teramura,[ab] S. Hosokawa,[ab] H. Kominami[c] and T. Tanaka[ab]

We found that plasmonic Au particles on titanium(IV) oxide (TiO₂) act as a visible-light-driven photocatalyst for overall water splitting free from any additives. This is the first report showing that surface plasmon resonance (SPR) in a suspension system effectively induces overall water splitting. Modification with various types of metal nanoparticles as co-catalysts enhanced the evolution of H₂ and O₂. Among these, Ni-modified Au/TiO₂ exhibited 5-times higher rates of H₂ and O₂ evolution than those of Ni-free Au/TiO₂. We succeeded in designing a novel solar energy conversion system including three elemental technologies, charge separation with light harvest and an active site for O₂ evolution (plasmonic Au particles), charge transfer from Au to the active site for H₂ production (TiO₂), and an active site for H₂ production (Ni cocatalyst), by taking advantage of a technique for fabricating size-controlled Au and Ni nanoparticles. Water splitting occurred in aqueous suspensions of Ni-modified Au/TiO₂ even under irradiation of light through an R-62 filter.

Although hydrogen (H₂) is primarily used in the chemical industry, it will become an important fuel in the near future. Production of H₂ from water by a semiconductor photocatalyst under photoirradiation of solar light has attracted significant attention because it offers a promising way to produce a clean, low-cost and environmentally friendly energy source.[1] Metal oxides as photocatalysts have been reported to be active for overall water splitting, but most of them require ultraviolet (UV) light (λ < 400 nm) because of the large bandgaps of semiconductor materials. However, UV light accounts for only about 5% of the total solar energy, whereas visible light accounts for about 50% of the total solar energy. The development of photocatalysts using visible light is an important topic from a practical point of view. Various visible light-responding photocatalysts, such as a solid solution of GaN and ZnO (GaN:ZnO)[2] and Z-type systems based on Pt/WO₃–Pt/ZrO/TaON[3] and BiVO₄–Ru/SrTiO₃:Rh,[4] have been reported for overall water splitting. To efficiently utilize solar energy, photocatalysts responding to longer wavelengths are required, and the design of photocatalysts working under green light (ca. 550 nm) and red light (ca. 620 nm) is a challenge. In addition, simple and additive-free water splitting systems, i.e., a system free from any chemicals except the photocatalyst and water, should be developed.

Nanoparticles of metals, such as copper (Cu), silver (Ag), and gold (Au), show strong photoabsorption (+light scattering) of visible light due to surface plasmon resonance (SPR). The resonance frequency of SPR is strongly dependent on the size, shape, interparticle interactions, dielectric properties, and local environment of the nanoparticles. Recently, plasmonic metal nanoparticles have been applied not only to stained glass but also to chemical sensors and biosensors,[5] surface-enhanced Raman scattering (SERS),[6] fluorescence enhancement,[7] and photocurrent enhancement in photovoltaic cells.[8] It has been reported that electron transfer from Au nanoparticles to a semiconductor occurred under irradiation of visible light (λ = ca. 550 nm) due to SPR.[9] Supported Au materials have been used as visible-light-responding photocatalysts for various chemical reactions,[10] including decomposition of organic substrates,[11] selective oxidation of an aromatic alcohol to a carbonyl compound,[12] H₂ formation from alcohols,[13] and reduction of organic compounds.[14] The research groups that reported these photocatalytic reactions concluded that the reactions are induced by SPR of the Au nanoparticles. In our previous study, we found that TiO₂ with both small metal nanoparticles and large Au particles shows activity for H₂ formation[15] and O₂ formation[16] with a sacrificial reagent such as 2-propanol and hexavalent chromium under irradiation of visible light.

[a]Department of Molecular Engineering, Graduate School of Engineering, Kyoto University, Kyotodaigaku Katsura, Nishikyo-ku, Kyoto 615-8510, Japan. E-mail: atsu.tana@apch.kindai.ac.jp

[b]Elements Strategy Initiative for Catalysts & Batteries (ESICB), Kyoto University, 1-30 Goryo-Ohara, Nishikyo-ku, Kyoto 615-8245, Japan

[c]Department of Applied Chemistry, Faculty of Science and Engineering, Kindai University, Kowakae, Higashiosaka, Osaka 577-8502, Japan

† Electronic supplementary information (ESI) available. See DOI: 10.1039/c6sc05135a

We have focused on an SPR-based photocatalyst powder for overall water splitting to H_2 and O_2 in an aqueous suspension without any sacrificial reagents or pH adjustment under irradiation of visible light. Recently, Zhong et al. developed photoelectric conversion and photoelectrochemical water splitting systems that use Au nanoparticles loaded onto a $SrTiO_3$ single-crystal photoelectrode irradiated by visible light.[17] In their study, the stoichiometric evolution of H_2 and O_2 was simultaneously obtained from two separate solution chambers with a chemical bias by regulating the pH values of the chambers. In the present study, we used an Au/TiO_2 sample for overall water splitting without using any reagents under irradiation of visible light. Here, we report that samples of Au/TiO_2 with co-catalysts were successfully prepared by a combination of photodeposition (PD) or impregnation (IM) and colloid photodeposition in the presence of hole scavenger (CPH) methods, and the samples exhibited larger H_2 and O_2 evolution rates than those of a co-catalyst-free Au/TiO_2 sample under the irradiation of visible light. Water splitting occurred in an aqueous suspension of Au/TiO_2 with NiO_x even under irradiation of light through an R-62 filter.

Fig. 1 shows the time courses of evolution of H_2 and O_2 from water over $Au(1.0)/TiO_2$ under a dark condition (0–3 h) or irradiation of visible light (3–24 h) in the absence of any additives. No gas evolved in the dark between 0 and 3 h, indicating that no thermocatalytic H_2 and O_2 formation occurred in the case of $Au(1.0)/TiO_2$. Just after irradiation with visible light, H_2 and O_2 evolved from the suspension of $Au(1.0)/TiO_2$. Since H_2 and O_2 increased linearly with the photoirradiation time, the rates of H_2 and O_2 evolution were determined to be 0.94 and 0.46 µmol h^{-1}, respectively. The overall photocatalytic reaction is expressed as eqn (1).

$$H_2O \rightarrow H_2 + \tfrac{1}{2}O_2 \qquad (1)$$

The ratio of moles of H_2 and O_2 (H_2/O_2 ratio) was calculated from eqn (2):

$$H_2/O_2 \text{ ratio} = n(H_2)/n(O_2), \qquad (2)$$
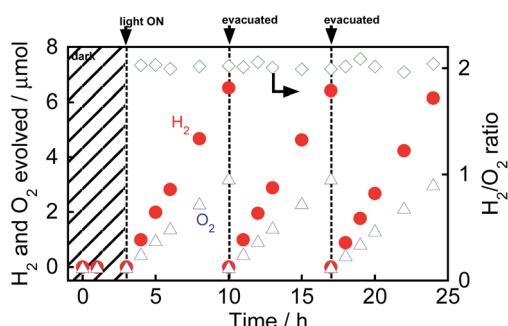
where $n(H_2)$ and $n(O_2)$ are the amounts of H_2 and O_2 during the photocatalytic reaction, respectively.

As shown in Fig. 1, the H_2/O_2 ratio was almost 2.0 regardless of the irradiation time, indicating that H_2 and O_2 evolution from water occurred with a high stoichiometry, as shown in eqn (1). To evaluate the stability of Au/TiO_2 in H_2 and O_2 production from water, Au/TiO_2 was used again. Irradiation with visible light of the reaction mixture again induced evolution of H_2 and O_2, and the formation continued from 10 to 17 h and from 17 to 24 h without deactivation.

It is known that the photocatalytic activity for overall water splitting over metal oxides is dependent on the presence of a co-catalyst.[18] Various co-catalysts were loaded onto TiO_2 using the PD method (Pt, Au, Pd, Rh, Ag) and IM method (Ni, Ru), and then, the Au particles were fixed on TiO_2–M using the CPH method. $Au(1.0)/TiO_2$–M(0.5) samples were used for evolution of H_2 and O_2 from water over various photocatalysts under visible light irradiation, and the effects of M on the reaction rates were compared. The amounts of H_2 and O_2 evolution for 4 h are shown in Table 1. The amounts of H_2 and O_2 evolution of all samples with co-catalysts, except for Pt, prepared in this study were larger than that of the M-free $Au(1.0)/TiO_2$ sample. Among the co-catalysts used in this study, Ni had the greatest effect on H_2 and O_2 evolution.

Fig. 2 shows the absorption spectra of TiO_2, TiO_2–NiO_x(0.5), $Au(1.0)/TiO_2$, and $Au(1.0)/TiO_2$–NiO_x(0.5) samples. The bare TiO_2 sample exhibited absorption only at $\lambda < 400$ nm because of the band gap excitation. Loading Ni species onto TiO_2 resulted in an increase in the baseline of the photoabsorption, which has generally been observed. In the spectra of the $Au(1.0)/TiO_2$ and $Au(1.0)/TiO_2$–NiO_x(0.5) samples, a strong photoabsorption was observed at around 550 nm, and it was attributed to SPR of the supported Au nanoparticles.[9–17] Since photoabsorption due to Ni species was also included, the $Au(1.0)/TiO_2$–NiO_x(0.5) sample exhibited stronger photoabsorptions at 700–800 nm.

Fig. 3(a) shows a TEM photograph of the TiO_2–NiO_x(0.5) sample simply prepared by the traditional IM method. NiO_x particles were observed, and the average diameter was determined to be 9.3 nm (Fig. S1(a)†), indicating that the NiO_x

Fig. 1 Time courses of evolution of H_2 and O_2 from water over $Au(1.0)/TiO_2$ under irradiation with visible light from a Xe lamp with an L-42 filter. After 10 h and 17 h of irradiation and evacuation, the suspension was irradiated again.

Table 1 Effect of modification of $Au(1.0$ wt%$)/TiO_2$ with various metal co-catalysts (0.5 wt%) on water splitting[a]

Cocat.	Modification method	Amount of products (4 h)/µmol	
		H_2	O_2
None	—	3.9	1.9
Pt	PD	2.7	1.1
Au		10	5.2
Pd		10	4.9
Rh		9.3	4.7
Ag		8.0	3.9
NiO_x	IM	22	11
RuO_x		6.1	3.0

[a] Reaction conditions: catalyst, 300 mg (co-catalyst-loaded); pure water, 300 cm^3, Xe lamp (300 W) with an L-42 filter; reaction vessel, Pyrex side-irradiation type.
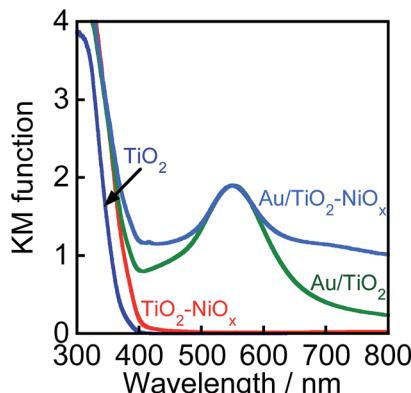
Fig. 2 Absorption spectra of TiO_2, $TiO_2-NiO_x(0.5)$, $Au(1.0)/TiO_2$, and $Au(1.0)/TiO_2-NiO_x(0.5)$.

Fig. 4 (a) Ni K-edge XANES spectra of Ni foil, NiO, $TiO_2-NiO_x(0.5)$ and $Au(1.0)/TiO_2-NiO_x(0.5)$; (b) XPS spectra of $Au(1.0)/TiO_2$, $TiO_2-NiO_x(0.5)$ and $Au(1.0)/TiO_2-NiO_x(0.5)$ around Ni 2p components.

particles were successfully deposited on the surface of TiO_2 using the IM method. Fig. 3(b) shows a TEM image of $Au(1.0)/TiO_2$ prepared by the CPH method using an Au colloidal solution. Gold particles were observed in the image, indicating that Au nanoparticles were deposited on the TiO_2 surface by the CPH method.

The average diameter of the Au particles in the sample was determined to be 13 nm (Fig. S1(b)†), which is in good agreement with the average diameter of the original colloidal Au nanoparticles before Au loading (Fig. S2†). In the TEM photograph of the $Au(1.0)/TiO_2-NiO_x(0.5)$ sample (Fig. 3(c)), both smaller and larger particles were observed, and the average diameters were determined to be 9.1 and 13 nm (Fig. S1(c and d)†), respectively. These results indicate that the CPH method induced no change in the NiO_x particles during the loading of the Au particles and that the Au particles were successfully loaded onto the TiO_2-NiO_x without a change in the original particle size, as in the case of loading Au onto bare TiO_2.[15]

Ni K-edge XANES spectra of $Au(1.0)/TiO_2-NiO_x(0.5)$ and $TiO_2-NiO_x(0.5)$ are shown in Fig. 4(a), for which Ni foil and NiO were used as references. The similar XANES spectra of Au/TiO_2-NiO_x, TiO_2-NiO_x and NiO clearly proves that the Ni species is

Fig. 3 TEM images of (a) $TiO_2-NiO_x(0.5)$, (b) $Au(1.0)/TiO_2$, and (c) $Au(1.0)/TiO_2-NiO_x(0.5)$.

NiO. X-ray photoelectron spectroscopy (XPS) was used to obtain information on the surfaces of the NiO_x co-catalysts in the Au/TiO_2-NiO_x samples. Normalized Ni 2p XPS spectra of $Au/TiO_2-NiO_x(0.5)$, $TiO_2-NiO_x(0.5)$, $Au(1.0)/TiO_2$ and TiO_2 are shown in Fig. S3,† of which the Ni 2p spectra have an overlap with the Auger parameters of Ti.[19] The subtracted XPS spectra obtained from the spectra of various samples (Au/TiO_2-NiO_x, TiO_2-NiO_x, Au/TiO_2) and TiO_2 are shown in Fig. 4(b). No peak is observed in the spectrum of Au/TiO_2. In the spectra of TiO_2-NiO_x and Au/TiO_2-NiO_x, peaks due to Ni ($2p_{3/2}$) that are assignable to Ni^{2+}, such as NiO, are observed at 856.3 eV.[20] On the other hand, peaks due to Ni ($2p_{3/2}$) that are assignable to Ni^0, such as Ni metal, are also observed at 852.7 eV (ref. 21) in the spectrum of Au/TiO_2-NiO_x. Although the corresponding change was not observed by XAFS measurement, partial formation of Ni metal is confirmed by the XPS spectrum, in which both signals assigned to Ni^{2+} and Ni^0 are observed. It is expected that the surface of NiO in the TiO_2-NiO_x is reduced to Ni metal during the deposition of the Au particles by the CPH method under irradiation with UV light. Fig. S4† shows the time courses of evolution of H_2 in methanol suspensions of $TiO_2-NiO_x(0.5)$ and $Au(1.0)/TiO_2-NiO_x(0.5)$ samples under irradiation with UV light. For the first hour, TiO_2-NiO_x showed a very low activity for H_2 evolution, and the continuous formation of H_2 at a constant rate was observed after the induction period. These results indicate that the state of the Ni species in TiO_2-NiO_x changes in the early stage of the photocatalytic reaction, *i.e.*, the surface of NiO in TiO_2-NiO_x was reduced to the Ni^0 species during the induction period. In contrast, there was no induction period for photocatalytic H_2 production over Au/TiO_2-NiO_x, indicating that some of the NiO_x particles had been reduced to metallic Ni.

In our previous study on the photocatalytic activity for H_2 formation from 2-propanol over Au/TiO_2-Pt samples, Pt exhibited the greatest effect on H_2 evolution.[15] The two types of metal particles had different functionalities, *i.e.*, the large Au particles contributed to the strong light absorption, and the small Pt particles acted as reduction sites for the H_2 evolution. However, the activity of the Au/TiO_2-Pt samples was much smaller than that of the other samples in this study, and the reaction rate gradually decreased (Fig. S5†), suggesting that the H_2-O_2 consumption reaction occurred on the Pt nanoparticles.

This was confirmed by testing the water formation reaction from a mixture of H_2 and O_2 in the dark using Au/TiO_2–Pt, as shown in Fig. 5(a). The amounts of H_2 and O_2 in a closed-gas circulation system decreased with time, indicating that water formation occurs on Au/TiO_2–Pt. On the other hand, Au/TiO_2–NiO_x and Au/TiO_2 samples showed a smaller rate of backward reaction between H_2 and O_2 into H_2O (consumption rates of H_2 and O_2) than that of the Au/TiO_2–Pt samples, as shown in Fig. 5(b and c). The small rate of the reverse reaction over Au/TiO_2 indicates that the formation of H_2 and O_2 was scarcely affected by the reverse reaction. Therefore, the reaction rate of H_2 and O_2 formation reflects the photocatalytic activity of Au/TiO_2 for water splitting. A linear relationship between the yields and time in Fig. 1, *i.e.*, zero-order kinetics, suggests that the reaction rate over Au/TiO_2 was determined by photon flux and photon utilization efficiency because the concentration of water on the Au/TiO_2 surface is constant. These results indicated that the actual rates of H_2 and O_2 evolution on the Au/TiO_2–Pt sample should be higher than those recorded by monitoring the gas phase of the reaction system. TiO_2, TiO_2–Pt(0.5), TiO_2–NiO_x(0.5), Au(1.0)/TiO_2, and Au(1.0)/TiO_2–NiO_x(0.5) samples were used for the evolution of H_2 and O_2 from water under visible light irradiation from a Xe lamp with an L-42 filter. The rates of H_2 and O_2 evolution are shown in Fig. S6.† No H_2 or O_2 was evolved in the case of TiO_2, TiO_2–Pt or TiO_2–NiO_x. These results indicate that the visible light coming from a filtered Xe lamp did not cause band gap excitation of TiO_2 and that photocatalysis and/or thermocatalysis of TiO_2–Pt and TiO_2–NiO_x were negligible under the present conditions. The Au(1.0)/TiO_2 sample, which was active in the overall water splitting, showed H_2 and O_2 evolution rates of 0.94 and 0.46 µmol h^{-1}, respectively. The Au(1.0)/TiO_2–NiO_x(0.5) sample exhibited much larger H_2 and O_2 formation rates of 5.5 and 2.7 µmol h^{-1}, respectively, indicating that the NiO_x co-catalyst loaded onto TiO_2 effectively acted as reduction sites for H_2 evolution. Loading both large Au particles and small co-catalyst particles on the TiO_2 surface without alloying or nanoparticle coagulation has been difficult, as stated above. This requisite was successfully achieved, and a large reaction rate was obtained, as predicted, by the Au/TiO_2–NiO_x sample prepared by the combination of the traditional IM method for NiO_x co-catalyst particles and the CPH method for large Au particles.
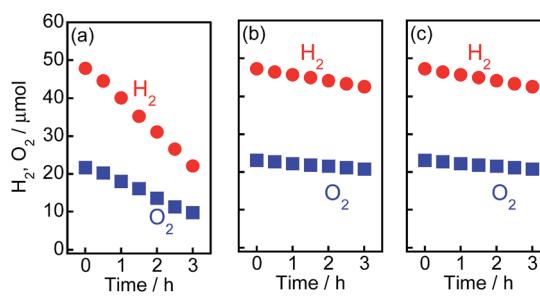
To examine the effect of the amount of Au on the rates of H_2 and O_2 formation, various amounts of Au(X) were loaded onto TiO_2–NiO_x(0.5) and TiO_2 samples using the CPH method. Au(X)/TiO_2–NiO_x(0.5) and Au(X)/TiO_2 samples were used for water splitting under irradiation of visible light, and the rates of H_2 and O_2 formation are shown in Fig. 6(a and b), respectively. The amounts of H_2 and O_2 increased linearly with the photo-irradiation time in all Au(X)/TiO_2–NiO_x(0.5) and Au(X)/TiO_2 samples, and the formation rates of H_2 and O_2 were determined from the slopes of the time-H_2 and O_2 evolution plots. The formation rates of H_2 and O_2 increased almost linearly with an increase in X until $X = 1.0$ wt% and gradually increased after $X = 1.0$ wt%. In a previous study,[15] the light absorption due to SPR at 550 nm of a sample prepared by the CPH method increased with an increase in Au loading until 1.0 wt% and gradually increased after $X = 1.0$ wt%. The Au loading dependency of the light absorption due to SPR was similar to that of the formation rates of H_2 and O_2, and a linear correlation was observed between the reaction rate and the light absorption due to SPR. We concluded that SPR photoabsorption by the Au particles was one of the important factors determining the photocatalytic activity in this study.

To examine the effect of the amount of the NiO_x co-catalyst on the rates of H_2 and O_2 formation, TiO_2–NiO_x(Y) samples with various Ni loadings (Y) were prepared, and Au particles (1.0 wt%) were introduced to the samples using the CPH method. The Au(1.0)/TiO_2–NiO_x(Y) samples were used for overall water splitting under irradiation of visible light; the rates of H_2 and O_2 formation are shown in Table 2. The Ni-free sample (Au(1.0)/TiO_2) exhibited small rates of H_2 and O_2 formation (0.94 and 0.46 µmol h^{-1}, respectively), as shown above. Only a small amount of NiO_x loading ($Y = 0.1$ wt%) increased the formation rate, indicating that the NiO_x co-catalyst effectively acted as the reduction center in the sample. The formation rate increased until $Y = 0.5$ wt%, and a further increase in Y decreased the formation rate. The maximum rates of H_2 and O_2 formation (5.5 and 2.7 µmol h^{-1}, respectively) were obtained at

Fig. 5 Water formation from H_2 and O_2 in the dark on (a) Au(1.0)/TiO_2–Pt(0.5), (b) Au(1.0)/TiO_2–NiO_x(0.5) and (c) Au(1.0)/TiO_2 samples. This experiment was carried out in pure water (300 cm^3) using a closed-gas circulation system containing a stoichiometric mixture of H_2 and O_2 gases.
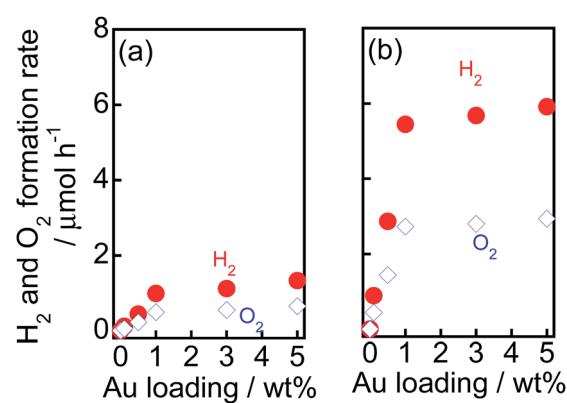
Fig. 6 Effect of Au loading amounts (X) on the rate of evolution of H_2 and O_2 from water over (a) Au(X)/TiO_2 and (b) Au(X)/TiO_2–NiO_x(0.5) samples under irradiation of visible light.

Table 2 Effect of $NiO_x(Y)$ loading amounts on the rate of evolution of H_2 and O_2 from water over $Au/TiO_2–NiO_x(Y)$ samples under irradiation of visible light

Entry	NiO_x loading (Y)/wt%	Size of NiO_x/nm	Formation rate/$\mu mol\ h^{-1}$	
			H_2	O_2
1	—	—	0.99	0.49
2	0.1	6.6	2.7	1.3
3	0.5	9.1	5.5	2.7
4	1.0	15	3.8	1.9
5	2.0	18	1.8	0.95

$Y = 0.5$ wt%. The average size of the NiO_x nanoparticles in $Au(1.0)/TiO_2–NiO_x(Y)$ was determined by TEM (Fig. S7†). NiO_x particles were loaded onto TiO_2 when the amount of NiO_x was small (<10 nm, $Y = 0.1$ and 0.5 wt%); however, the size of the NiO_x particles drastically increased to 15 nm at $Y = 1.0$ wt%, indicating that the IM method was suitable for loading a small amount of small particles on TiO_2. Since the particle size of NiO_x with $Y = 0.5$ was smaller (<10 nm) than that with $Y > 1.0$ and the concentration of the Ni species with $Y = 0.5$ was higher than that with $Y = 0.1$, the photocatalytic activity of the $Au(1.0)/TiO_2–NiO_x(0.5)$ samples was higher than those of the other samples. These results suggested that the NiO_x particles acted as reduction sites in the $Au(1.0)/TiO_2–NiO_x(Y)$ samples and that the reaction is sensitive to the structure of the NiO_x particles.

Fig. 7 shows time courses of the evolution of H_2 and O_2 from water over $Au(1.0)/TiO_2–NiO_x(0.5)$ under a dark condition (0–5 h) or irradiation with visible light from a Xe lamp with L-42 (5–13 h, 29–37 h) or O-54 (13–21 h) or R-62 (21–29 h). Fig. 7 is different from an ordinary action spectrum, and the results indicate the effects of both the wavelength of light and amount of photons. No gas was evolved in the dark between 0 and 5 h, indicating that no thermocatalytic H_2 and O_2 formation occurred in the case of $Au(1.0)/TiO_2–NiO_x(0.5)$. The value of H_2/O_2 was almost 2.0 regardless of the irradiation time and the cut-off filter used. The formation rates of H_2 and O_2 decreased with an increase in the filter number (L-42 > O-54 > R-62), corresponding to the decrease in photoabsorption (Fig. S8(a)†). It should be noted that water


Fig. 7 Time courses of evolution of H_2 and O_2 from water over $Au(1.0)/TiO_2–NiO_x(0.5)$ under irradiation of visible light from a Xe lamp with various filters. After 13, 21 and 29 h of irradiation and evacuation, the suspension was irradiated again.

splitting continuously occurred, even under irradiation of light through an R-62 filter. To the best of our knowledge, this is the first report showing H_2 and O_2 formation from water splitting free from any additives over an Au plasmonic photocatalyst under irradiation of red light (>>600 nm). Irradiation of visible light from a Xe lamp with L-42 to the reaction mixture again induced evolution of H_2 and O_2 from water, and the formation continued from 29 to 37 h without deactivation after irradiation of visible light from different cut-off filters.

Other research groups also reported H_2 formation[13a,22a] and O_2 formation[22] over Au/TiO_2 in the presence of a sacrificial reagent under irradiation of visible light, indicating that Au/TiO_2-related materials have a sufficient potential for H_2 formation (H^+/H_2: 0 V NHE pH 0) and oxidization of H_2O (H_2O/O_2: 1.23 V NHE pH 0). Therefore, the simultaneous evolution of H_2 and O_2 by water splitting in this study is reasonable and is attributed to the acceleration of the positive reaction and suppression of the reverse reaction by co-catalysts introduced to Au/TiO_2. Energy (ca. 2.5 or 2.1 eV) corresponding to light ($\lambda = ca.$ 500 nm or 600 nm) that the Au/TiO_2 materials absorb is reasonably large for both H_2 and O_2 formations even though some over-potentials are required for these formations. In our previous study, we examined the action spectra in H_2 formation[15] and O_2 formation[16] over $Au/TiO_2–Pt$ in the presence of sacrificial reagents under irradiation with visible light and reported that both spectra showed a similar tendency of absorption spectra. Since rates of water splitting were very small under the irradiation of weak monochromated light, we analyzed the results shown in Fig. 7, and the intensity of the light coming through the cut-off filters is shown in Fig. S8(a).† From the results, the difference in the intensity of light irradiated to $Au(1.0)/TiO_2–NiO_x$ was calculated in three ranges (Fig. S8(b)†). Based on the incident photons from 520 to 650 nm and the difference in the formation rates in the case of O54 and R62, the value of the apparent quantum efficiency (AQE) was calculated to be 0.013%. In the same way, the values of AQE were calculated based on the incident photons in other ranges and plotted against the wavelength of light irradiated to $Au(1.0)/TiO_2–NiO_x$ as well as that of AQE from 520 to 650 nm. As shown in Fig. S9,† the wavelength-dependency of AQE was roughly consistent with the spectrum of $Au(1.0)/TiO_2$. We think that this action spectrum is direct evidence that the plasmon-induced water splitting is really induced over $Au(1.0)/TiO_2–NiO_x$. As shown in the action spectrum (Fig. S9†), the upper limit of light wavelength available for water splitting over $Au/TiO_2–NiO_x$ seems to be ca. 700 nm (corresponding to ca. 1.8 eV).

Based on the proposed working mechanism for H_2 and O_2 formation in the presence of a sacrificial reagent, the expected energy diagram and working mechanism for H_2 and O_2 formation from water over $Au/TiO_2–NiO_x$ under irradiation with visible light are shown in Scheme 1. Four processes would occur: (1) the incident photons are absorbed by Au particles through their SPR excitation,[10] (2) electrons are injected from the Au particles into the conduction band of TiO_2, (3) the resultant electron-deficient Au particles oxidize H_2O to O_2 and return to their original metallic state, and (4) electrons in the conduction band of TiO_2 transfer to the NiO_x nanoparticles
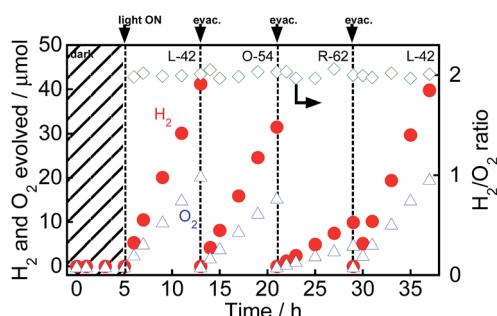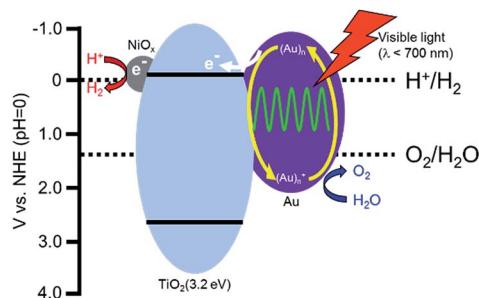
Scheme 1 Expected reaction mechanism for the production of H_2 and O_2 from water over a Au/TiO$_2$–NiO$_x$ sample.

as a co-catalyst at which reduction of H^+ to H_2 occurs. Rapid electron transfer from Au to the TiO$_2$ film under visible light irradiation was observed using femtosecond transient absorption spectroscopy.[9b] In addition to O_2 evolution in the presence of a sacrificial reagent,[22] Shi *et al.* demonstrated enhancement in the photocurrent generation and photocatalytic water oxidation sensitized by Au showing SPR under irradiation with visible light.[23] Process (3) is supported by these results. Reduction of H^+ by electrons in the conduction band of TiO$_2$ is difficult because the level is very close to the reduction potential. Therefore, continuous evolution of H_2 is generally achieved by introducing a co-catalyst on TiO$_2$. The co-catalyst effect observed in this study supports process (4). As shown in Fig. 1 and Table 1, Au(1.0)/TiO$_2$ evolved H_2 and O_2, indicating that Au particles loaded by the CPH method also work as a co-catalyst. We also prepared Au-loaded tin(IV) oxide (SnO$_2$) and Au/SnO$_2$–NiO$_x$ using the CPH method, and used it for water splitting under the same conditions. Evolution of H_2 and O_2 over these samples was negligible because the level of the conduction band of SnO$_2$ is positive to the potential for H^+ reduction, *i.e.*, insufficient for H^+ reduction. The difference in the results between TiO$_2$ and SnO$_2$ indirectly supports process (4).

Conclusions

The Au/TiO$_2$ sample continuously yielded H_2 and O_2 from water in the absence of additives under visible light irradiation. Au/TiO$_2$ with NiO$_x$ particles was successfully prepared by the combination of photodeposition and impregnation methods. We observed that modification of the Au/TiO$_2$ sample with Ni drastically improved the performance of the photocatalyst, and the samples continuously split water even under irradiation with red light. The backward reaction between the evolved H_2 and O_2 into H_2O could be suppressed using NiO$_x$, although the Pt co-catalyst enhanced the consumption rates and H_2 and O_2. These results suggest that separate loading of the NiO$_x$ co-catalyst without alloying with Au particles is effective for enhancing the activity of an Au plasmonic photocatalyst for overall water splitting.

Experimental section

Commercial TiO$_2$ powder (P25, 50 m^2 g^{-1}) with an anatase/rutile phase was supplied by Degussa.

Loading of the co-catalysts (M: Pt, Au, Pd, Rh, Ag) on TiO$_2$ (preparation of TiO$_2$–M) was performed by the PD method. TiO$_2$ powder was suspended in 10 cm^3 of an aqueous solution of methanol (50 vol%) in a test tube, and the test tube was sealed with a rubber septum under argon (Ar). An aqueous solution of the co-catalyst source was injected into the sealed test tube and then photoirradiated for 2 h at λ > 300 nm by a 400 W high-pressure mercury arc (Eiko-sha, Osaka) with magnetic stirring in a water bath continuously kept at 298 K. The co-catalyst source was reduced by photogenerated electrons, and metal was deposited on the surface of the TiO$_2$ particles. Analysis of the liquid phase after photodeposition revealed that the co-catalyst source had been almost completely (>99.9%) deposited on the TiO$_2$ particles. The resultant powder was washed repeatedly with distilled water and then dried at 310 K overnight under air.

Loading of co-catalysts (M: Ni, Ru) on TiO$_2$ (preparation of TiO$_2$–M) was performed by the IM method. TiO$_2$ powder was suspended in 10 cm^3 of an aqueous solution of a co-catalyst source in a glass dish and was evaporated to dryness at 333 K. The product was dried overnight at room temperature and then calcined at 573 K for 1 h in air.

Colloidal Au nanoparticles were prepared using the method reported by Frens.[24] To 750 cm^3 of an aqueous tetrachloroauric acid (HAuCl$_4$) solution (0.49 mmol dm^{-3}), 100 cm^3 of an aqueous solution containing sodium citrate (39 mmol dm^{-3}) was added. The solution was heated and boiled for 1 h. After the color of the solution changed from deep blue to deep red, the solution was boiled for an additional 30 min. After the solution was cooled to room temperature, Amberlite MB-1 (ORGANO, 60 cm^3) was added to remove excess sodium citrate. After 1 h of treatment, MB-1 was removed from the solution using a glass filter. Loading of Au particles on the TiO$_2$–M samples was performed by the CPH method.[25] Preparation of TiO$_2$–M having 1.0 wt% Au as a typical sample is described. A TiO$_2$–M sample (168 mg) was suspended in 20 cm^3 of an aqueous solution of colloidal Au nanoparticles (0.085 mg cm^{-3}) in a test tube, and the test tube was sealed with a rubber septum under Ar. An aqueous solution of oxalic acid (50 μmol) was injected into the sealed test tube. The mixture was photoirradiated at λ > 300 nm by a 400 W high-pressure mercury arc under Ar with magnetic stirring in a water bath continuously kept at 298 K. The resultant powder was washed repeatedly with distilled water and then dried at 310 K overnight under air. Co-catalyst-free samples (Au/TiO$_2$) were also prepared by the same method using bare TiO$_2$ samples. When samples with different Au contents were prepared, the amount of TiO$_2$–M (or TiO$_2$) was changed (volume and concentration of the Au colloidal solution being fixed). Hereafter, an Au-loaded TiO$_2$–M sample having Y wt% of M and X wt% of Au is designated as Au(X)/TiO$_2$–M(Y); for example, a sample having 0.5 wt% Ni and 1.0 wt% Au is shown as Au(1.0)/TiO$_2$–NiO$_x$(0.5). Oxalic acid is necessary for complete Au loading on TiO$_2$ (ref. 25) and may protect citrate from covering Au particles. Since the numbers of co-catalyst particles was much larger than that of Au particles,[15] the co-catalysts will act effectively.

Diffuse reflectance spectra of the samples were obtained with a JASCO Corporation V-670 spectrometer equipped with an

integrating sphere. Spectralon, which was supplied by Labsphere Inc., was used as a standard reflection sample such as $BaSO_4$. The morphology of the samples was observed under a JEOL JEM-2100F transmission electron microscope (TEM) operated at 200 kV at the Joint Research Center of Kindai University. X-ray photoelectron spectroscopy (XPS) measurements were conducted on an ESCA-3400 spectrometer (Shimadzu, Japan). A sample was mounted on a silver sample holder using conductive carbon tape and was analyzed using Mg Kα radiation in a vacuum chamber in 0.1 eV steps. The position of the carbon peak (284.6 eV) for C 1s was used to calibrate the binding energy for all the samples. Ni K-edge (8.3 keV) X-ray absorption fine structure (XAFS) measurements were made in the fluorescence mode at the BL01B1 beamline of the SPring-8 synchrotron radiation facility (Hyogo, Japan). A typical data reduction procedure (*e.g.*, background removal or normalization) was carried out with Athena (version 0.9.20).

Reactions were conducted in a Pyrex side-irradiation vessel connected to a glass closed gas circulation system. A 300 mg sample of Au/TiO_2–M powder was dispersed in pure water (300 cm^3) using a magnetic stirrer, and this reactant solution was evacuated under vacuum several times to completely remove any residual air. Following this, a small amount of Ar gas was introduced into the reaction system prior to irradiation under a 300 W xenon lamp (Cermax, PE300BF) filtered with various filters with a 15 A output current. The amounts of H_2 and O_2 in the gas phase were measured using a Shimadzu GC-8A gas chromatograph equipped with an MS-5A column.

Acknowledgements

References

1 (a) A. Kudo and Y. Miseki, *Chem. Soc. Rev.*, 2009, **38**, 253; (b) R. Abe, *J. Photochem. Photobiol., C*, 2010, **11**, 179; (c) X. Chen, S. Shen, L. Guo and S. S. Mao, *Chem. Rev.*, 2010, **110**, 6503.

2 (a) K. Maeda, K. Teramura, D. Lu, T. Takata, N. Saito, Y. Inoue and K. Domen, *Nature*, 2006, **440**, 295; (b) K. Maeda, K. Teramura, D. Lu, N. Saito, Y. Inoue and K. Domen, *Angew. Chem., Int. Ed.*, 2006, **45**, 7806.

3 K. Maeda, M. Higashi, D. Lu, R. Abe and K. Domen, *J. Am. Chem. Soc.*, 2010, **132**, 5858.

4 (a) Y. Sasaki, H. Nemoto, K. Saito and A. Kudo, *J. Phys. Chem. C*, 2009, **113**, 17536; (b) Y. Sasaki, H. Kato and A. Kudo, *J. Am. Chem. Soc.*, 2013, **135**, 5441.

5 M. E. Stewart, C. R. Anderton, L. B. Thompson, J. Maria, S. K. Gray, J. A. Rogers and R. G. Nuzzo, *Chem. Rev.*, 2008, **108**, 494.

6 P. L. Stiles, J. A. Dieringer, N. C. Shah and R. P. Van Duyne, *Annu. Rev. Anal. Chem.*, 2008, **1**, 601.

7 J. R. Lakowicz, K. Ray, M. Chowdhury, H. Szmacinski, Y. Fu, J. Zhang and K. Nowaczyk, *Analyst*, 2008, **133**, 1308.

8 H. A. Atwater and A. Polman, *Nat. Mater.*, 2010, **9**, 205.

9 (a) Y. Tian and T. Tatsuma, *J. Am. Chem. Soc.*, 2005, **127**, 7632; (b) A. Furube, L. Du, K. Hara, R. Katoh and M. Tachiya, *J. Am. Chem. Soc.*, 2007, **129**, 14852.

10 (a) M. Xiao, R. Jiang, F. Wang, C. Fang, J. Wang and J. C. Yu, *J. Mater. Chem. A*, 2013, **1**, 5790; (b) S. C. Warren and E. Thimsen, *Energy Environ. Sci.*, 2012, **5**, 5133; (c) X. Zhou, G. Liu, J. Yu and W. Fan, *J. Mater. Chem.*, 2012, **22**, 21337; (d) S. Linic, P. Christopher and D. B. Ingram, *Nat. Mater.*, 2011, **10**, 911; (e) T. Tatsuma, *Bull. Chem. Soc. Jpn.*, 2013, **86**, 1.

11 E. Kowalska, R. Abe and B. Ohtani, *Chem. Commun.*, 2009, 241.

12 (a) S. Naya, M. Teranishi, T. Isobe and H. Tada, *Chem. Commun.*, 2010, **46**, 815; (b) A. Tanaka, K. Hashimoto and H. Kominami, *J. Am. Chem. Soc.*, 2012, **134**, 14526–14533.

13 (a) H. Yuzawa, T. Yoshida and H. Yoshida, *Appl. Catal., B*, 2012, **115**, 294; (b) A. Tanaka, S. Sakaguchi, K. Hashimoto and H. Kominami, *Catal. Sci. Technol.*, 2012, **2**, 907.

14 (a) X. Ke, S. Sarina, J. Zhao, X. Zhang, J. Chang and H. Zhu, *Chem. Commun.*, 2012, **48**, 3509; (b) A. Tanaka, Y. Nishino, S. Sakaguchi, T. Yoshikawa, K. Imamura, K. Hashimoto and H. Kominami, *Chem. Commun.*, 2013, **49**, 2551.

15 A. Tanaka, S. Sakaguchi, K. Hashimoto and H. Kominami, *ACS Catal.*, 2013, **3**, 79.

16 A. Tanaka, K. Nakanishi, R. Hamada, K. Hashimoto and H. Kominami, *ACS Catal.*, 2013, **3**, 1886.

17 Y. Zhong, K. Ueno, Y. Mori, X. Shi, T. Oshikiri, K. Murakoshi, H. Inoue and H. Misawa, *Angew. Chem., Int. Ed.*, 2014, **53**, 10350.

18 K. Maeda, *J. Photochem. Photobiol., C*, 2011, **12**, 237.

19 G. M. Ingo, S. Dire and F. Babonneau, *Appl. Surf. Sci.*, 1993, **70**, 230.

20 A. N. Mansour, *Surf. Sci. Spectra*, 1994, **3**, 231.

21 A. N. Mansour, *Surf. Sci. Spectra*, 1994, **3**, 211.

22 (a) C. G. Silva, R. Juarez, T. Marino, R. Molinari and H. Garcia, *J. Am. Chem. Soc.*, 2011, **133**, 595; (b) A. Primo, T. Marino, A. Corma, R. Molinari and H. Garcia, *J. Am. Chem. Soc.*, 2011, **133**, 6930.

23 X. Shi, K. Ueno, N. Takabayashi and H. Misawa, *J. Phys. Chem. C*, 2013, **117**, 2494.

24 G. Frens, *Nature Phys. Sci.*, 1973, **241**, 20.

25 A. Tanaka, A. Ogino, M. Iwaki, K. Hashimoto, A. Ohnuma, F. Amano, B. Ohtani and H. Kominami, *Langmuir*, 2012, **28**, 13105.